

Stochastic multicomponent reactive transport analysis of
low quality drainage release from waste rock piles:
controls of the spatial distribution of acid generating and
neutralizing minerals

Daniele Pedretti^{a,b}, K. Ulrich Mayer^a, Roger D. Beckie^a

^a*Earth, Ocean and Atmospheric Sciences, University of British Columbia (UBC),
Vancouver (BC) Canada*

^b*Geological Survey of Finland (GTK), Espoo, Finland (daniele.pedretti@gtk.fi)*



Stochastic multicomponent reactive transport analysis of
low quality drainage release from waste rock piles:
controls of the spatial distribution of acid generating and
neutralizing minerals

Abstract

In mining environmental applications, it is important to assess water quality from waste rock piles (WRPs) and estimate the likelihood of acid rock drainage (ARD) over time. The mineralogical heterogeneity of WRPs is a source of uncertainty in this assessment, undermining the reliability of traditional bulk indicators used in the industry. We focused in this work on the bulk neutralizing potential ratio (NPR), which is defined as the ratio of the content of non-acid-generating minerals (typically reactive carbonates such as calcite) to the content of potentially acid-generating minerals (typically sulfides such as pyrite). We used a streamtube-based Monte-Carlo method to show why and to what extent bulk NPR can be a poor indicator of ARD occurrence. We simulated ensembles of WRPs identical in their geometry and bulk NPR , which only differed in their initial distribution of the acid generating and acid neutralizing minerals that control NPR . All models simulated the same principal acid-producing, acid-neutralizing and secondary mineral forming processes. We show that small differences in the distribution of local NPR values or the number of flow paths that generate acidity strongly influence drainage pH. The results indicate that

the likelihood of ARD (epitomized by the probability of occurrence of $\text{pH} < 4$ in a mixing boundary) within the first 100 years can be as high as 75% for a $NPR=2$ and 40% for $NPR=4$. The latter is traditionally considered as a "universally safe" threshold to ensure non-acidic waters in practical applications. Our results suggest that new methods that explicitly account for mineralogical heterogeneity must be sought when computing effective (upscaled) NPR values at the scale of the piles.

Keywords: multicomponent reactive transport, mineralogical heterogeneity, stochastic analysis, acid rock drainage, waste rock piles, neutralizing potential ratio

1. Introduction

In environmental mining assessments, one critical aspect to control is whether a waste rock pile (WRP) has a high or low effective neutralizing capacity, which reflects its overall (bulk) ability to buffer the acidity produced within the pile. Low effective neutralizing capacity can imply deleterious properties characteristic of acid rock drainage (ARD), e.g. $\text{pH} < 4$ and high sulfate and metal concentrations in the pile's outflow. (e.g. INAP-GARD, 2014; Morin and Hutt, 1997; Parbhakar-Fox and Lottermoser, 2015; Price, 2009).

Bulk indicators are typically used in the industry to predict whether a WRP will possess a high or low effective neutralizing capacity. A widely-adopted and well-known indicator is the bulk neutralizing potential ratio (NPR), which is based on the acid-base accounting originally developed by Sobek et al. (1978). NPR is obtained from laboratory-based analysis of n_l

15 rock samples obtained from the site as

$$NPR = \frac{1}{n_l} \sum_{i=1}^{n_l} \frac{NP_i}{AP_i} \quad (1)$$

16 where NP is a measure of the total mass of minerals available in the sample
17 to neutralize the acidity, typically carbonates, and is expressed as equiv-
18 alent kg CaCO_3 , and AP is a measure of total mass of acid producing
19 minerals, typically sulfides, also expressed in equivalents kg of CaCO_3 (to
20 be directly comparable with NP). Theoretically, $NPR > 1$ indicates that
21 after complete reaction of the sample minerals the resulting solution will not
22 be acidic, while $NPR < 1$ indicates that after complete reaction of the sam-
23 ple minerals the resulting solution will be acidic. Unfortunately, measuring
24 $NPR > 1$ does not necessarily translate into a WRP with high effective neu-
25 tralizing capacity. Indeed, ARD guidelines (e.g. Price, 2009) suggest that
26 $NPR > 2$ would ensure a limited occurrence of acidic drainage from a pile,
27 while $NPR > 4$ seems a well-established *universal* threshold to ensure no
28 occurrence of acidic drainage. A value between $NPR = 1$ and $NPR = 4$
29 falls in the so-called "gray" or uncertain zone.

30 We highlight here some reasons to explain why laboratory-based bulk
31 indicators such as the NPR are not always useful criteria to determine if
32 drainage may become acidic at some point in the future. First, it shall be
33 considered that WRPs are unsaturated and usually highly heterogeneous
34 deposits (Eriksson and Destouni, 1997; Eriksson et al., 1997; Fala et al.,
35 2013; Amos et al., 2014; Lahmira and Lefebvre, 2014; Lahmira et al., 2016)
36 in which the formation and control of ARD depends on a large number of

37 nonlinear, coupled physical, chemical and biological processes (e.g. Amos
38 et al., 2009; Blowes et al., 2003; Lefebvre et al., 2001; Nicholson et al., 1990;
39 Nordstrom, 2011; Pedretti et al., 2015; Lorca et al., 2016). Static chemical
40 tests, such as the Sobek test, and small-scale kinetic tests, such as kinetic
41 or humidity cells, do not properly account for all processes occurring under
42 field conditions, and have been seen to significantly overestimate the reaction
43 rates of weathering processes (e.g. Malmström et al., 2000).

44 As defined in (1), the bulk NPR can be seen as a crude homogenization
45 based on a simple arithmetic averaging of NP and AP from samples col-
46 lected from the site and analyzed in the laboratory. The bulk NPR does
47 not account for the spatial variability of minerals within the WRPs, while
48 the neutralizing capacity of WRPs may be controlled not only by the bulk
49 amount of AP and NP minerals in the system, but also by their specific
50 sequence along a flow path, as discussed for instance by Morin and Hutt
51 (2000). Indeed, in geochemically heterogeneous systems, the water quality
52 at the end of a flow path depends in part on the sequence of minerals encoun-
53 tered along the flow path (e.g. Palmer and Cherry, 1984). Thus, the spatial
54 distribution of minerals in the piles, which are ubiquitously heterogeneous,
55 may have an important control on pile drainage.

56 Since the exact distribution of the phases that contribute to NP and
57 AP within WRPs is never known in practice, the prediction of ARD from
58 WRPs becomes uncertain. Stochastic models handling this type of *epis-*
59 *temic* uncertainty (e.g. Tartakovsky and Winter, 2008) are not yet common
60 for studies on WRPs. One reason is due to the intense computational bur-
61 den required to solve for multidimensional multicomponent Eulerian-based

62 reactive transport in heterogeneous WRPs (e.g. Demers et al., 2013; Fala
63 et al., 2013; Lahmira and Lefebvre, 2014; Lahmira et al., 2016). Alternative
64 computationally efficient methods, such as streamtube-based or Lagrangian
65 models (e.g. Bellin et al., 1994; Finkel et al., 2002; Simmons et al., 1995;
66 Thiele et al., 1996; Yabusaki et al., 1998), can be however adopted. For
67 instance, Eriksson and Destouni (1997) used a Lagrangian approach to in-
68 vestigate the impact of preferential flow on a WRP in Sweden, previously
69 analyzed by Strömberg and Banwart (1994). Malmström et al. (2004) used
70 Lagrangian models for ARD formation and evolution in the context of mine
71 tailings.

72 In this work we use a streamtube-based approach to develop a full Monte-
73 Carlo analysis and quantify the role of the spatial distribution of minerals
74 for a fixed bulk NPR on the formation of ARD in WRPs through time.
75 Each streamtube is modeled using the multicomponent reactive transport
76 code MIN3P (Mayer et al., 2002), which simulates the main acid-producing,
77 acid-neutralizing and secondary mineral forming processes in unsaturated
78 systems. The stochastic modeling allows explaining how, under the same
79 bulk NPR , the spatial distribution of NP and AP phases affects the likeli-
80 hood of water acidification in WRPs. We focus on those bulk NPR values
81 that are traditionally considered in the gray zone (e.g. $NPR = 2$), as well as
82 larger values ($NPR = 4, 10$) which are traditionally considered safe thresh-
83 olds according to mine water guidelines (e.g. Price, 2009). Our purpose is
84 to highlight and study the key difference between "local" and "bulk" NPR
85 values, the first defined as the ratio of NP and AP in a lab-scale sample
86 collected at a specific location of the pile, the second defined as the ratio of

87 *NP* and *AP* of all the minerals in the entire pile.

88 **2. Problem statement**

89 We create stochastic realizations of WRPs within which we simulate
90 unsaturated flow and reactive transport. We use a simplified conceptual
91 model (Figure 1) to study in detail the effects of the spatial distribution of
92 *NP* and *AP* minerals in WRPs. The model is an idealization that contains
93 the essential features that allow us to isolate the effects of the variability in
94 local *NPR* values on the resulting drainage composition.

95 Each pile realization is conceptualized as a 2D profile 100 m long and 10
96 m high. One batter is located on the right side of the pile with a $\theta = 37^\circ$
97 angle of repose, similar to the tipping phases (TP) and batters of real-
98 world WRPs (e.g. Azam et al., 2007). Conceptually, a TP is similar to
99 a geological depositional facies. Within each TP, the waste rock can be
100 either characterized by similar mineralogical composition and abundance,
101 assuming all rock in a TP is extracted from the same geological formation
102 of the mine, or a more heterogeneous composition, due to natural geological
103 heterogeneity of the rock formation, as well as internal segregation, layering
104 and blending during pile construction (e.g. INAP-GARD, 2014).

105 We assume that the piles initially contain two reactive primary min-
106 eral phases, pyrite and calcite. Pyrite represents the most common sulfide
107 mineral undergoing oxidation and generating acidity and provides a major
108 source of *AP*. Calcite represents a carbonate mineral that buffers acidity
109 and provides a major source of *NP*. Weathering of these two minerals can
110 give rise to the formation of secondary mineral phases such as gypsum and

111 ferrihydrite, providing solubility controls for Ca, SO₄ and Fe. Secondary
112 minerals can form at any point and moment within the pile. Oxygen and
113 carbon dioxide partial pressures remain in constant equilibrium with atmo-
114 spheric conditions throughout the pile and for the entire simulation time,
115 representing a well-ventilated system (e.g. Amos et al., 2009; Lefebvre et al.,
116 2001). Sulfide oxidation is therefore not limited by the amount of oxygen,
117 and similarly calcite dissolution is not affected by the accumulation of car-
118 bon dioxide within the pile (e.g. Lorca et al., 2016). Non-reactive minerals
119 make up the bulk of the pile such that physical properties like porosity and
120 permeability do not change in time as reactions occur. All these processes
121 are accounted for in our simulations. The equations defining the geochemical
122 system are reported as Supplementary Information (SI).

123 To isolate the effect of heterogeneous mineral distribution without the
124 potentially complicated and non-trivial effects associated with different trans-
125 port rates within the pile (e.g. Eriksson and Destouni, 1997), we assume
126 hydraulic homogeneity in the WRPs. Unsaturated flow is driven by a wet-
127 dry seasonal recharge rate which is applied uniformly across the crown and
128 batter of the pile. The base of the pile is assumed to be impermeable, where
129 pile drainage is collected to form a composite mixed drainage, as shown
130 in Figure 1. Multiple observations made on WRPs suggest that the pile
131 drainage is made up of well-defined sub-vertical flow paths, in some cases
132 resulting in a preferential-like flow regime (e.g. Amos et al., 2014; Blackmore
133 et al., 2014; Nichol et al., 2005; Peterson, 2014; Smith and Beckie, 2003). It
134 is reasonable to expect that mixing of the multiple flow paths composing the
135 system's drainage at the control plane dominates compared to local mixing

136 occurring inside the piles along the flow paths or across the flow paths by
137 transverse dispersion, as observed in saturated porous systems (e.g. Rahman
138 et al., 2005).

139 Under these conditions, a stochastic streamtube (ST) modeling approach
140 is a reasonable and computationally-efficient approximation for the simula-
141 tion of multidimensional multicomponent reactive transport within hetero-
142 geneous WRPs under uncertainty. The stochastic analysis is based on the
143 solution of Monte-Carlo simulations of ensembles of correlated random spa-
144 tial fields or realizations and analysis of the statistics of the model outputs.
145 Within each realization, the ST approach is used to solve for reactive trans-
146 port, as conceptualized in Figure 1. Without lack of generality, it is assumed
147 that flow occurs along vertical one-dimensional (1D) STs, whose hydraulic
148 properties are fixed, as reported in the SI. While mixing occurs exclusively
149 at the base of the pile, we note that in the ST approach the mixing layer
150 does not necessarily need to be located at the base of the pile. It could also
151 be located, for example, on top of a continuous capillary barrier within the
152 piles, such as a traffic surface, giving rise to localized mixing of water and/or
153 a lateral spring from the WRPs (e.g. Fala et al 2013).

154 **3. Methodology**

155 *3.1. Generation of mineralogical random fields*

156 We start by generating independent identically distributed (i.i.d.) ran-
157 dom fields of volumetric fractions (ϕ) of pyrite and calcite. Each field has the
158 same spatial statistics, including the same spatially averaged or bulk NPR ,
159 and represents a possible spatial map of NP and AP minerals within the

160 pile. The volume fractions are adopted by MIN3P to define the amount of
161 minerals in the model (SI) and can be related to wt% by simple conversion
162 based on mineral densities and porosities.

163 To build random realizations of mineralogical assemblage, we utilize the
164 Sequential Indicator Simulation (SIS) geostatistical algorithm (Emery, 2004;
165 Goovaerts, 2000; Journel and Alabert, 1990; Soares, 1998) coded in SGEMS
166 (Remy et al., 2009). For a specific mineral, each SIS simulation requires
167 three variables: the spatially-averaged mineral volume fraction ($\bar{\phi}$), the vari-
168 ance (σ_{ϕ}^2) and the correlation function (C_{ϕ}). In all realizations we use an
169 exponential covariance of the form

$$C_{\phi}(\theta_C) = \sigma_{\phi}^2 \exp\left(-\frac{d}{a(\theta_C)}\right) \quad (2)$$

170 where d is the distance between two points, θ_C is an angle oriented along
171 one of the axes of the anisotropic covariance ellipsoid, and a is the range
172 of the correlation along that direction. The ratio between $a(\theta_C)$ and the
173 dimension of the domain along θ_C provides a measure of the continuity of
174 the mineralogical content the direction θ_C .

175 We generate unconditioned 2D random fields of size 100 m \times 10 m and
176 a discretization of 1 m \times 1 m (for a total number of cells $n_c=1000$ per
177 field) replicating heterogeneous distributions of pyrite and calcite content in
178 mineralogically heterogeneous WRPs. The grid resolution is assumed to be
179 sufficient to capture the variability of the heterogeneity in the waste rock,
180 and is similar to the one adopted in other studies involving numerical models
181 of heterogeneous waste rocks (e.g. Lahmira and Lefebvre, 2014; Lahmira

182 et al., 2016).

183 We formulate four different ensembles of simulations, each of which is
184 characterized by a different bulk NPR value (0.5, 2, 4, 10) but identical
185 coefficient of variance ($CV = \sqrt{\sigma_\phi^2/\bar{\phi}}$). We set $CV=0.6$, a value that maxi-
186 mizes the variability of mineral content in each realization without generat-
187 ing physically unrealistic negative ϕ values. We set ranges $a_1=10$ m along
188 the major axis, parallel with the orientation of the waste rock tipping phases
189 at an angle of $\theta_C = \theta = 37^\circ$, and $a_2=5$ m along the perpendicular minor
190 axis at an angle of $\theta_C = 127^\circ$. At the scale of individual waste rock particles
191 (grid blocks), we postulate an inverse correlation between the sulfide con-
192 tent and the carbonate content with an intermediate correlation coefficient
193 $\rho = 0.5$. This selection is made to account for the expected lower sulfide
194 content in carbonate-rich rocks (and vice-versa) with statistical uncertainty
195 or noise.

196 An example of the random fields generated using this methodology and
197 parameters is shown in Figure 2. It can be observed that the resulting
198 spatial distributions are heterogeneous, with discrete zones having similar
199 NPR values along the vertical direction. The vertical homogeneity is the
200 result of using $a_1 = 10$ m, which generates a relatively continuity of the same
201 mineral amount (i.e. same ϕ) along the TP dipping angle. This approach
202 is representative for a single tip from haul trucks, where the load comes
203 from one location in the mine. The lateral variability is the result of using
204 $a_2 = 5$ m, which is lower than the lateral extension of the pile (100m).

205 Using the same approach, we generate an ensemble of 100 random fields
206 of pyrite and 100 for calcite for each bulk NPR value, each with a distinct

207 spatial distribution of *NP* and *AP* minerals but same statistical distribu-
208 tions. The arbitrary number of simulations serves us to obtain a represen-
209 tative ensemble of results to evaluate the likelihood of low-quality drainage,
210 as described in Section 4.2.

211 *3.2. Reactive transport along each ST*

212 For each realization of the ensemble, we simulate drainage chemistry
213 over 1000 years along all individual STs in the pile. A succinct description
214 of the flow and reactive transport model is provided here. Additional details
215 about the model setup, boundary conditions as well as flow and transport
216 parameters used in the analysis can be found in the SI.

217 Each realization consists of $N_{ST}=100$ STs, each of which was subdivided
218 into cells of 1 m length, 1 m width, a cross sectional area $A=1\text{ m}^2$ and a
219 volume of 1 m^3 . The total pile discharge area at the pile base is 100 m^2 .
220 Below the crown the ST contains 10 cells, while below the batter the num-
221 ber of cells decreases as the pile thins towards the toe (as conceptualized in
222 Figure 1). The number of STs is deemed adequate to evaluate the impact
223 of geochemical heterogeneity on the long-term outflow geochemistry, while
224 maximizing the efficiency of the model calculations. A sensitivity analysis
225 reported in the SI confirms the adequacy of the selected vertical grid res-
226 olution against numerical dispersion, leaving the mineralogical distribution
227 unchanged.

228 The saturated hydraulic conductivity and Van Genuchten unsaturated
229 properties are homogeneous and isotropic at each point of the domain. The
230 selected hydraulic parameters (SI) ensure that there is no surface ponding

231 and that the outflow discharge rate from each ST (Q) is controlled by the
232 recharge rates assigned at the top of each ST (q_r) and A . To simulate a
233 wet-dry seasonality, each year a uniform daily recharge rate equivalent to
234 $q_r=1000$ mm/y is applied for six months, followed by six months of $q_r=0$.
235 Because q_r and A are constant in all STs, the maximum flow rate per ST
236 is $Q = 3.17 \times 10^{-8}$ m³/s during the wet season , while the minimum flow
237 rates approach zero during the dry season. A prescribed concentration flux
238 is defined at the surface, while a free-exit concentration boundary is set at
239 the base. The recharge and initial pore-water composition within the pile
240 have low solute concentrations, as reported in the SI.

241 To focus exclusively on the effect of the distribution of NP and AP
242 minerals, we set homogeneous pyrite oxidation rates described by a simple
243 zero-order kinetic model. This is a simplification of the actual nature of the
244 process, which is actually better described by surface-area and pH-controlled
245 mineral weathering rates (e.g. Park and Levenspiel, 1975), but not accounted
246 for in this work for computational reasons. We set a representative effective
247 rate coefficient of $k = 10^{-9}$ mol L⁻¹s⁻¹, which is in range of values found by
248 Nicholson et al. (1990) using a shrinking core model. A sensitivity analysis
249 (not reported) showed however that a different k does not substantially
250 affect our conclusions. Geochemical calculations utilize a thermodynamic
251 database derived from WATEQ4F (Ball and Nordstrom, 1991). We refer
252 to Mayer et al. (2002) for details on the thermodynamic constants. The
253 geochemical model accounts for all dissolved species associated with the
254 components forming calcite, pyrite, water, oxygen and carbon dioxide. The
255 principal secondary mineral phases defined by these elements are allowed

256 to precipitate within a grid block when saturated. Calcite, gypsum and
257 ferrihydrite are treated as in quasi-equilibrium conditions and allowed to
258 precipitate and (re)dissolve.

259 3.3. *Mixing*

260 Mixing of waters at the base of the pile from the multiple STs is com-
261 puted in two steps. The first step consists in the algebraic calculation of
262 concentration of components (j) exfiltrating from each streamtube (i) at the
263 last day of each wet season (τ_l , where $l = 1, \dots, 1000$ corresponds to each
264 simulated year). A flux-averaged component concentration $T_F(j, \tau_l)$ is cal-
265 culated as

$$T_F(j, \tau_l) = \sum_{i=1}^{N_{ST}} w(i) T_j(i, j, \tau_l) \quad w(i) = \frac{Q_i(\tau_l)}{Q(\tau_l)} \quad (3)$$

266 For instance, $T_F(SO_4, \tau_1)$ is the mixed concentration of sulfate at the base
267 of the pile at the last day of the first wet season; $T_F(SO_4, \tau_2)$ is the concen-
268 tration at last day of the second wet season; and so on.

269 The second step uses MIN3P to calculate the geochemistry of the mixed
270 basal drainage. Mixing calculations are performed under the assumption of
271 equilibrium with atmospheric O_2 and CO_2 and no precipitating secondary
272 minerals in the mixing boundary. The concentrations of the components,
273 pH and alkalinity in the mixed waters are quantified and it is assumed that
274 the resulting water discharged from from underneath the pile immediately
275 after mixing. Alkalinity is calculated following the formulation of MINTEQ
276 (Felmy et al., 1984).

277 The assumptions of no precipitating secondary minerals and a once-per-
278 year mixing are made to increase the computational efficiency in light of the
279 large number of simulations generated within the Monte Carlo framework.
280 A sensitivity analysis, reported in the SI, reveals that mixing calculations
281 performed on a daily basis and/or allowing secondary minerals (gypsum and
282 ferrihydrite) to precipitate do not qualitatively affect the resulting model
283 outputs and the conclusions of this work. It is noted that while mixing of
284 components is computed once annually, flow and reactive transport along
285 the STs are still computed continuously over the 1000 simulated years, with
286 variable time steps spanning from 10^{-10} day to 1 day , utilizing the adaptive
287 time stepping algorithm of MIN3P (Mayer and MacQuarrie, 2010).

288 4. Results & Analysis

289 4.1. Analysis of individual realizations

290 The results from two selected realizations (Figure 2) chosen from the
291 ensemble with bulk $NPR=2$ are shown in Figure 3 .

292 The first key element to observe is that, in both realizations, the ma-
293 jority of the STs (gray lines) do not generate ARD. In realization 1 about
294 80% of the STs show low sulfate concentrations, with $pH \approx 6.5$ and elevated
295 alkalinity. The remaining 20% of STs, however, display typical ARD-like
296 conditions, with high sulfate concentrations and low pH, with minimum
297 pH-values 2-3. Consistently, in these STs the alkalinity drops below zero
298 (i.e. representing acidity) during the low pH stages. In realization 2, the
299 number of ARD-like STs is about 10% of the total. This number is slightly
300 lower than in realization 1 and graphically distinguishable in Figure 3 by

301 the lower density of STs characterized by sulfate concentration peaks and
302 low pH values.

303 The number of acidic STs in the realization strongly affects the compo-
304 sition of the basal mixed drainage in each simulation. In realization 1, the
305 mixed drainage shows $\text{pH} < 4$ over extended periods of time (about 100-150
306 years since the beginning of the simulations), dropping to lows of $\text{pH} \approx 4$,
307 which corresponds to lows in alkalinity and a peak in sulfate concentrations.
308 After 150-200 years, the pile rapidly recovers to circumneutral values, while
309 sulfate concentrations tend to gradually decrease towards a stable value. In
310 realization 2, at the initial stages the composite drainage is characterized by
311 generally higher alkalinity (i.e. less acidity) than in realization 1, with less
312 pronounced peaks of sulfate and $\text{pH} > 4$ for most of the simulation time.

313 Over short and intermediate time scales (< 300 years), the spatial config-
314 uration of mineral abundances seems to have an important control on basal
315 drainage chemistry. Indeed, there are pronounced differences in the com-
316 posite drainage of the two realizations which can be uniquely related to the
317 different number of acidic STs, and are thus ascribable exclusively to min-
318 eralogical heterogeneity. While the majority of ST drainage waters show
319 circumneutral pH in the simulations, some STs can reach acidities much
320 higher than the maximum alkalinities in neutral STs. The solubility of car-
321 bonates limits the alkalinity of carbonate-saturated water to hundreds of
322 mg/L, whereas sulfide oxidation has no mineral solubility control and acidi-
323 ties can reach thousands of mg/L. Thus, the higher acidities of the acidic
324 STs dominate the basal drainage chemistry despite being a minority of the
325 total STs.

326 These first observations explain why it can be difficult to predict the
327 actual neutralizing capacity of WRPs in presence of mineralogical hetero-
328 geneity. Just a small subset of STs releasing ARD was seen to be responsible
329 for the acidification of the entire drainage collected from the base. More-
330 over, the fact that the majority of STs is circumneutral is not a sufficient
331 condition to ensure that the resulting mixed drainage will be circumneutral.

332 For upscaling purposes, it is possible that the same results would equally
333 hold if mixing accounts only for those streamtubes that more actively con-
334 tribute to basal discharge and solute loadings. Here, we can find some
335 analogies between the effect of the spatial distribution of minerals on the
336 resulting mixed drainage and the effect of flow heterogeneity documented by
337 Eriksson et al. (1997). They concluded that because of flow by-passing and
338 preferential flow, only 55%-70% of the pile's rock effectively contributed to
339 the loadings from the WRP. Thus, the effect of flow channeling by Eriksson
340 et al. (1997) results in a fraction of the waste rocks that actually contribute
341 to the pile's overall behavior observed at a control section. We note however
342 that the combined effect of mineral and flow heterogeneities is not yet well
343 understood and requires further investigation.

344 Over the long term (>300 years), the total sulfate concentrations become
345 comparable in the two piles and the pH tends to approach circumneutral
346 values. This occurs because at long time scales the pyrite is almost en-
347 tirely oxidized in the two piles and sulfate release is only associated with
348 gypsum dissolution. Gypsum precipitates and accumulates in most stream-
349 tubes in both realizations during the active phase of sulfide oxidation and
350 redissolves later on, therefore yielding a relatively homogeneous release of

351 SO_4 . In real WRPs, several more minerals can exist in the piles, including
352 slower-reacting aluminosilicates, which can provide pH buffering over time
353 scales longer than carbonates. While the behavior of real WRPs will thus
354 differ somewhat from our results, our conclusions about the effect of mineral
355 distribution on composite outflow chemistry at short and intermediate time
356 scales (<300 years) will not. Indeed, the variability in outflow chemistry be-
357 tween realizations here is fundamentally driven by the different distribution
358 of minerals, and any changes in geochemical assumptions should affect all
359 realizations in approximately the same way.

360 4.2. Monte-Carlo simulations

361 From each realization, a unique mixed drainage chemistry time series is
362 produced using MIN3P and the approach described in Section 3.3. One time
363 series reflects only possible random outcome from the ensemble of results be-
364 longing to a specific NPR value. In the following, we examine the likelihood
365 or probability of occurrence of a particular value of mixed-drainage pH at
366 given times by analyzing the statistics from the ensemble of results from
367 each bulk NPR .

368 We first analyze the ensemble results for the case with bulk $NPR=2$. In
369 Figure 4, the histograms represent the frequency of the mixed-drainage pH
370 from the individual realizations. In the plots the y-axis scale is limited to a
371 density of 0.25 in all panels to emphasize the difference among the different
372 cases. The red lines represent the empirical cumulative density function,
373 which can be interpreted as the probability (P) that the mixed drainage pH
374 falls below a certain value. Using P , we can define a likelihood of occurrence

375 (L) as

$$L = P(\text{pH} < \text{pH}^*) \quad (4)$$

376 which is the proportion of scenarios in which the mixed-drainage pH is below
377 a threshold of compliance pH^* . As a working assumption, we describe the
378 results based on $\text{pH}^* < 4$.

379 Figure 4 shows that as the piles evolve geochemically over time, the
380 relative frequency of specific pH values in the composite drainage changes.
381 The results highlight that bulk $NPR = 2$ is rarely a sufficient condition
382 to expect neutralized drainage from WRPs within short and intermediate
383 time scales. For instance, after 25 years in the majority of simulations the
384 composite drainage shows $\text{pH} \approx 3-4$, while it only remains circumneutral in a
385 limited subset of the simulations. At 25 years, the probability curve suggests
386 that the likelihood of $\text{pH} < 4$ is $L \approx 90\%$, i.e. 90 out of 100 realizations with
387 bulk $NPR=2$ yield a composite drainage with $\text{pH} < 4$. The likelihood of
388 not exceeding the selected $\text{pH}^*=4$ is still 75% after one century since the
389 placement of the WRPs. The likelihood drops to lower values after 150 years,
390 where it stabilizes around $L=30\%$, and remains almost identical, even after
391 300 years. Results not plotted here suggest that likelihood drops to very
392 low values ($L < 5\%$) for very large time scales (1000 years).

393 The histograms and cumulative distributions for bulk NPR scenarios are
394 shown in Figure 5, including the guidelines-recommended $NPR = 4$ (Price,
395 2009). In addition to the line representing the selected threshold $\text{pH}^*=4$,
396 we plot the lines corresponding to $L=50\%$ and $L=5\%$. For $NPR=0.5$, the

397 likelihood of water acidification increases compared with the case $NPR=2$.
398 This result is not surprising and in line with the expected behavior of a
399 WRP with a lower calcite-to-pyrite ratio and thus with a lower probability
400 of pH buffering.

401 Surprisingly, for $NPR=4$ we found that the likelihood is still $L \approx 70\%$ at
402 50 years and $L \approx 40\%$ at 100 years. After 150 years the number of simula-
403 tions with $pH < 4$ drops, with $L \approx 15\%$. We thus found that $NPR=4$ is not a
404 reliable threshold to ensure good quality drainage water from a WRP with
405 similar characteristics as those simulated in this work, questioning the valid-
406 ity of $NPR=4$ as a *universal* indicator to predict poorly acidified drainage
407 exfiltrating waste rock piles.

408 A higher NPR than 4 is needed to ensure low likelihood of water not
409 exceeding the threshold pH^* . For instance, the results for $NPR=10$ show it
410 to be a much safer criterion than $NPR=4$, although we did not carry out
411 simulations for intermediate NPR values that may provide similar results.

412 **Summary & Conclusion**

413 We present and discuss the results from a stochastic modeling approach
414 where we study the effects of heterogeneous mineral distributions on the
415 likelihood of acid drainage from WRPs for different bulk NPR values. To
416 allow a more direct interpretation of our results, we adopt some simplifi-
417 cations compared to real sites, such as homogeneous flow conditions and
418 no control of silicate weathering on the long term. Gas transport is not
419 rate-limited in our simulations.

420 We account for the mineral content (volumetric fractions) as the effective

421 property controlling the variability of drainage quality exfiltrating the piles.
422 We do not explicitly correlate mineralogical reactivity and particle size, for
423 instance assigning a higher reaction rates to smaller size. Instead, we assume
424 that a high-content mineral zone means both higher amount of *NP* or *AP*
425 mineral and a higher reactivity for the minerals present in the zones. For
426 instance, it can be seen as a zone enriched in minerals with high surface
427 areas. Vice-versa, a low content mineral zone contains with a lower fraction
428 of *NP* or *AP* minerals with a lower reactivity.

429 We show that, for the conceptual model developed in this analysis,
430 WRPs with bulk *NPR*=2 generate drainage pH<4 after 100 years with
431 a probability of about 75%. Unexpectedly, after 100 years this probability
432 is still about 40% when bulk *NPR*=4. In other terms, two out of five WRPs
433 with bulk *NPR*=4 are expected to generate poor-quality pH<4 drainage af-
434 ter 100 years. This aspect should be take into account by decision makers,
435 as *NPR*=4 is generally considered a safe criterion when operating WRPs
436 (Price, 2009).

437 The Monte-Carlo result is explained considering the results from individ-
438 ual realizations from the ensemble. In two geostatistical simulations having
439 bulk *NPR* \approx 2 we observe that the composite drainage can give rise to either
440 acidic or circumneutral drainage because of a limited subset of streamtubes
441 (flow paths) discharging at a mixing plane and undergoing acidic conditions.
442 For upscaling purposes, the impact of mineralogical heterogeneity can be
443 seen as qualitative similar to the behavior of hydraulic heterogeneity and
444 preferential flow described by Eriksson and Destouni (1997). Only a sub-
445 set of streamtubes effectively contribute to the pile-average composition of

446 the exfiltrating drainage, depending on concentration loadings and acid-
447 ity/alkalinity. These results suggest one possible way towards a correct
448 upscaling of the effective neutralizing capacity of mineralogically heteroge-
449 neous waste rock piles.

450 **Acknowledgments**

451 The authors acknowledge the useful comments by the Editor (Dr.Micheal
452 Annable) and one anonymous reviewer, which helped improving the qual-
453 ity of the manuscript. All the data and additional information used and
454 cited in this paper can be provided by the corresponding author (DP) at
455 specific requests. This research was enabled in part by support provided
456 by WestGrid (www.westgrid.ca) and Compute Canada / Calcul Canada
457 (www.computecanada.ca).

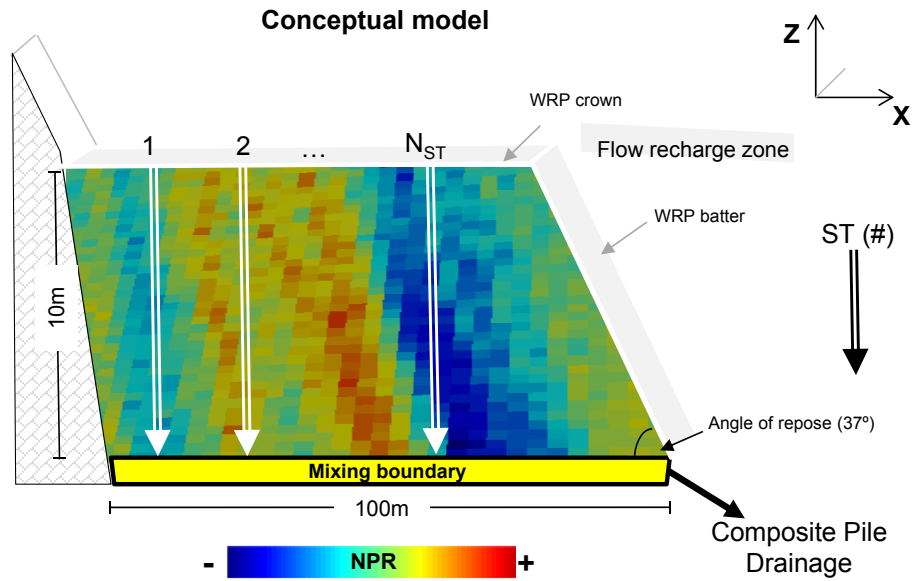


Figure 1: Conceptual model of the problem analyzed in this work. From the recharge zones (crown and batter), water infiltrates into the pile forming multiple hydraulically-homogeneous streamtubes (STs). Each ST intercepts a random sequence of minerals, and in turn a random sequence of NPR zones. For a specific realization, the composition of the resulting WRP drainage depends on the flux-averaged concentration of each ST being collected at the control plane (mixing boundary at base of the pile). The composition of each ST at the control plane, and in turn of the composite drainage, depends on the specific sequence of minerals encountered in each realization.

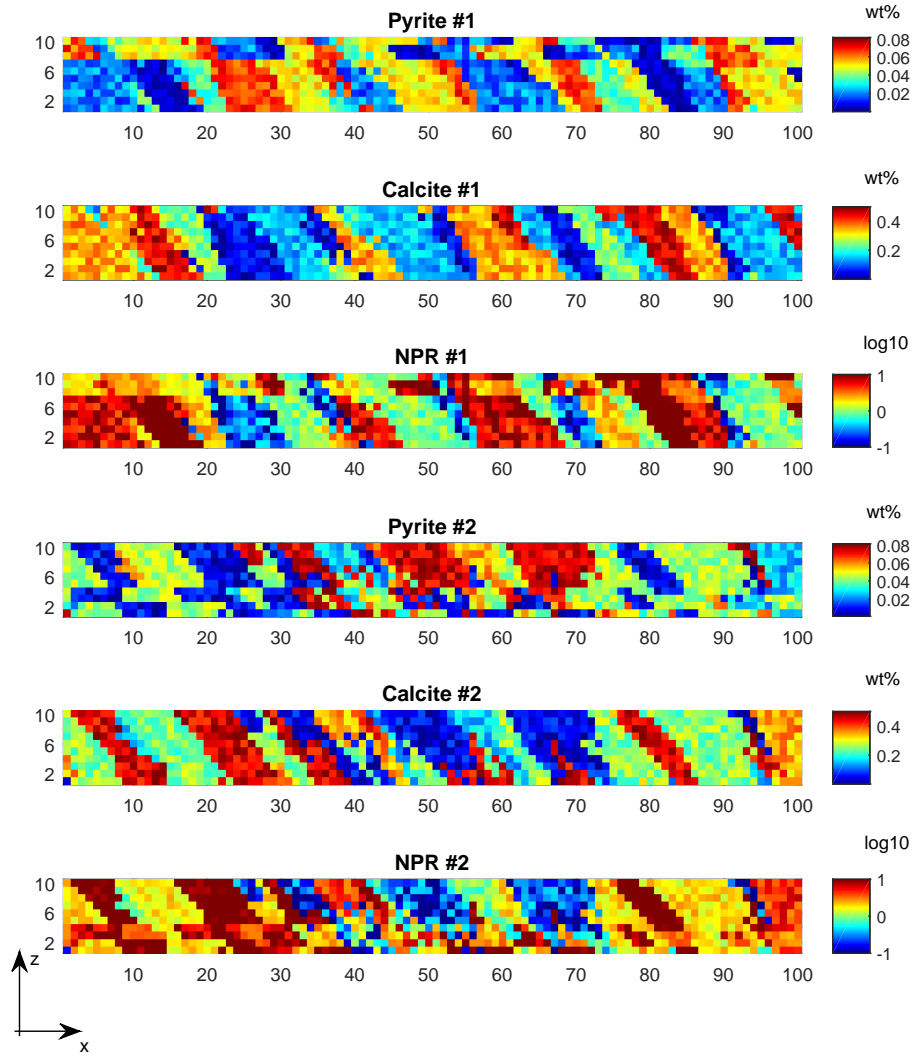


Figure 2: Two example realizations or maps of initial mineral distributions. The average dip along the major axis is parallel with the angle of repose of the waste rock ($\theta = 37^\circ$).

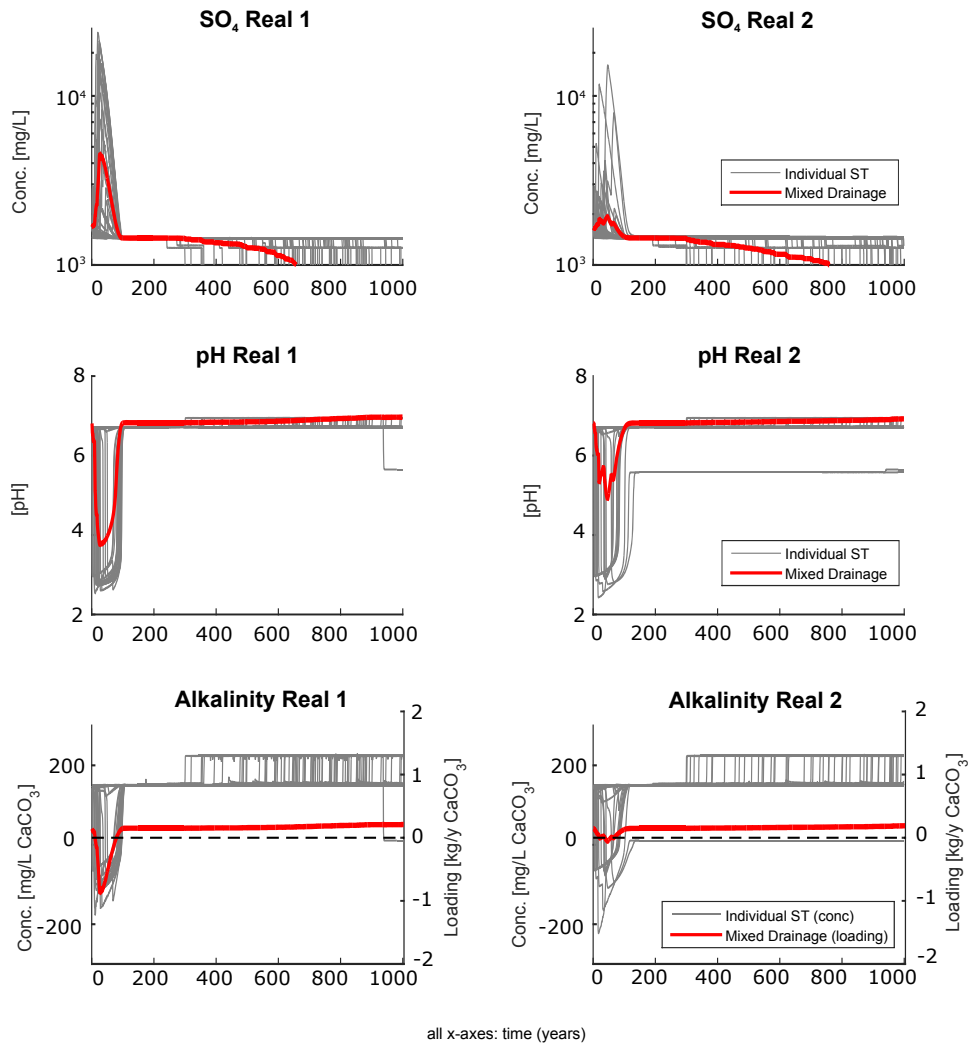


Figure 3: Analysis of two individual realizations with bulk $NPR=2$. The geometry, flow field, bulk properties and boundary conditions are identical in both realizations. They differ only in the organization of primary minerals (calcite and pyrite) within the piles, which generates a heterogeneous distribution of local NPR values. The dotted lines highlights zero alkalinity. The red line indicated the mixing values calculated using MIN3P (see Section 3.3).

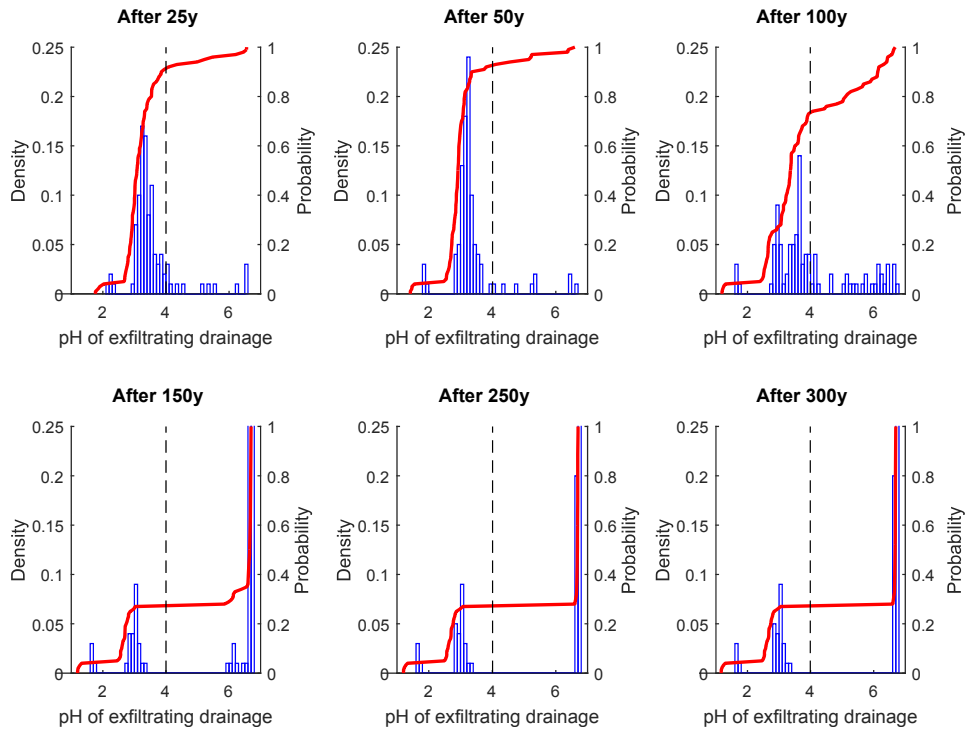


Figure 4: Ensemble results of the mixed-drainage pH from the scenarios with bulk $NPR = 2$ at different times. The vertical dotted line emphasizes $pH=4$, an arbitrary value selected to estimate the likelihood (L) of the piles to generate low-quality drainage.

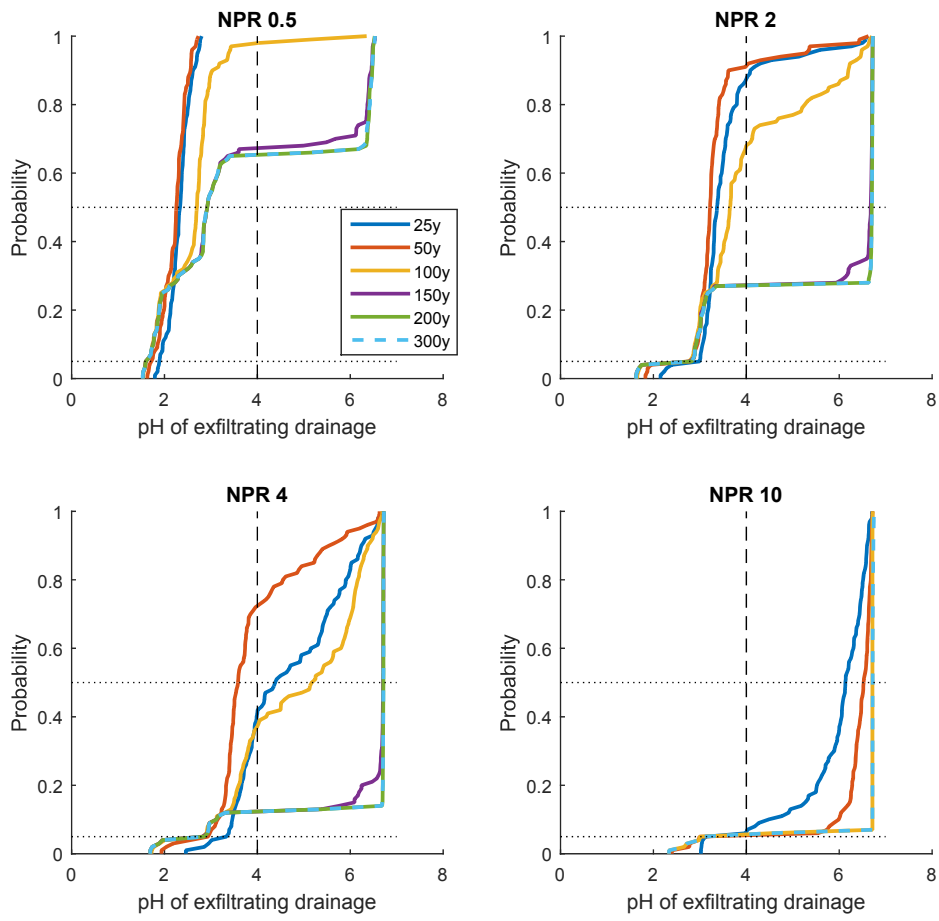


Figure 5: Comparison of ensemble results from different bulk NPR values, at different times. All panels show the pH of the mixed drainage from 100 random simulations. In each individual simulation, pH is calculated using the mixing approach described in Section 3.3.

458 **References**

- 459 Amos, R.T., Blowes, D.W., Bailey, B.L., Segó, D.C., Smith, L., Ritchie,
460 A.I.M., 2014. Waste-rock hydrogeology and geochemistry. *Applied Geo-*
461 *chemistry* doi:10.1016/j.apgeochem.2014.06.020.
- 462 Amos, R.T., Blowes, D.W., Smith, L., Segó, D.C., 2009. Measurement of
463 Wind-Induced Pressure Gradients in a Waste Rock Pile. *Vadose Zone*
464 *Journal* 8, 953. doi:10.2136/vzj2009.0002.
- 465 Azam, S., Wilson, G., Herasymuk, G., Nichol, C., Barbour, L., 2007. Hy-
466 drogeological behaviour of an unsaturated waste rock pile: a case study
467 at the Golden Sunlight Mine, Montana, USA. *Bulletin Of Engineering*
468 *Geology And The Environment* 66, 259–268.
- 469 Ball, J., Nordstrom, D., 1991. WATEQ4F – User’s manual with revised
470 thermodynamic data base and test cases for calculating speciation of ma-
471 jor, trace and redox elements in natural waters. USGS Numbered Series
472 90-129.
- 473 Bellin, A., Rubin, Y., Rinaldo, A., 1994. Eulerian-Lagrangian approach for
474 modeling of flow and transport in heterogeneous geological formations.
475 *Water Resources Research* 30, 2913–2924. doi:10.1029/94WR01489.
- 476 Blackmore, S., Smith, L., Ulrich Mayer, K., Beckie, R.D., 2014. Comparison
477 of unsaturated flow and solute transport through waste rock at two exper-
478 imental scales using temporal moments and numerical modeling. *Journal*
479 *of Contaminant Hydrology* 171, 49–65. doi:10.1016/j.jconhyd.2014.10.009.

480 Blowes, D., Ptacek, C., Jambor, J., Weisener, C., 2003. The Geochemistry of
481 Acid Mine Drainage, in: *Treatise on Geochemistry*. Elsevier, pp. 149–204.

482 Demers, I., Molson, J., Bussire, B., Laflamme, D., 2013. Numerical modeling
483 of contaminated neutral drainage from a waste-rock field test cell. *Applied*
484 *Geochemistry* 33, 346–356. doi:10.1016/j.apgeochem.2013.02.025.

485 Emery, X., 2004. Properties and limitations of sequential indicator simula-
486 tion. *Stochastic Environmental Research and Risk Assessment* 18, 414–
487 424. doi:10.1007/s00477-004-0213-5.

488 Eriksson, N., Destouni, G., 1997. Combined effects of dissolution kinetics,
489 secondary mineral precipitation, and preferential flow on copper leaching
490 from mining waste rock. *Water Resources Research* 33, 471–483.

491 Eriksson, N., Gupta, A., Destouni, G., 1997. Comparative analysis of
492 laboratory and field tracer tests for investigating preferential flow and
493 transport in mining waste rock. *Journal of Hydrology* 194, 143–163.
494 doi:10.1016/S0022-1694(96)03209-X.

495 Fala, O., Molson, J., Aubertin, M., Dawood, I., Bussire, B., Chapuis,
496 R.P., 2013. A numerical modelling approach to assess long-term un-
497 saturated flow and geochemical transport in a waste rock pile. *Inter-*
498 *national Journal of Mining, Reclamation and Environment* 27, 38–55.
499 doi:10.1080/17480930.2011.644473.

500 Felmy, A., Girvin, D., Jenne, E., 1984. MINTEQA—a Computer Program for
501 Calculating Aqueous Geochemical Equilibria.

- 502 Finkel, M., Liedl, R., Teutsch, G., 2002. Modelling Reactive Transport of
503 Organic Solutes in Groundwater with a Lagrangian Streamtube Approach,
504 in: (DFG), D.F. (Ed.), *Geochemical Processes*. Wiley-VCH Verlag GmbH
505 & Co. KGaA, pp. 115–134.
- 506 Goovaerts, P., 2000. Geostatistical approaches for incorporating elevation
507 into the spatial interpolation of rainfall. *Journal of Hydrology* 228, 113–
508 129. doi:10.1016/S0022-1694(00)00144-X.
- 509 INAP-GARD, 2014. GARD (Global Acid Rock Drainage) Guide
510 The International Network for Acid Prevention (INAP). URL:
511 <http://www.gardguide.com/>.
- 512 Journal, A.G., Alabert, F.G., 1990. New Method for Reservoir Mapping.
513 *Journal of Petroleum Technology* 42, 212–218. doi:10.2118/18324-PA.
- 514 Lahmira, B., Lefebvre, R., 2014. Numerical modelling of transfer processes in
515 a waste rock pile undergoing the temporal evolution of its heterogeneous
516 material properties. *International Journal of Mining, Reclamation and*
517 *Environment* 0, 1–22. doi:10.1080/17480930.2014.889362.
- 518 Lahmira, B., Lefebvre, R., Aubertin, M., Bussire, B., 2016. Effect of het-
519 erogeneity and anisotropy related to the construction method on transfer
520 processes in waste rock piles. *Journal of Contaminant Hydrology* 184,
521 35–49. doi:10.1016/j.jconhyd.2015.12.002.
- 522 Lefebvre, R., Hockley, D., Smolensky, J., Lamontagne, A., 2001. Multiphase
523 transfer processes in waste rock piles producing acid mine drainage: 2.

- 524 Applications of numerical simulation. *Journal of Contaminant Hydrology*
525 52, 165–186. doi:10.1016/S0169-7722(01)00157-7.
- 526 Lorca, M.E., Mayer, K.U., Pedretti, D., Smith, L., Beckie, R.D., 2016. Spa-
527 tial and Temporal Fluctuations of Pore-Gas Composition in Sulfidic Mine
528 Waste Rock. *Vadose Zone Journal* 15. doi:10.2136/vzj2016.05.0039.
- 529 Malmström, M.E., Destouni, G., Banwart, S.A., Strömberg, B.H.E., 2000.
530 Resolving the Scale-Dependence of Mineral Weathering Rates. *Environ-
531 mental Science & Technology* 34, 1375–1378. doi:10.1021/es990682u.
- 532 Malmström, M.E., Destouni, G., Martinet, P., 2004. Modeling Expected So-
533 lute Concentration in Randomly Heterogeneous Flow Systems with Mul-
534 ticomponent Reactions. *Environmental Science & Technology* 38, 2673–
535 2679. doi:10.1021/es030029d.
- 536 Mayer, K.U., Frind, E.O., Blowes, D.W., 2002. Multicomponent reactive
537 transport modeling in variably saturated porous media using a generalized
538 formulation for kinetically controlled reactions. *Water Resources Research*
539 38, 13–1–13–21. doi:10.1029/2001WR000862.
- 540 Mayer, K.U., MacQuarrie, K.T.B., 2010. Solutions of the MoMaS reactive
541 transport benchmark with MIN3P - model formulation and simulation
542 results. *Computational Geosciences* 14, 405-419.
- 543 Morin, K.A., Hutt, N., 1994. An empirical technique for predicting the
544 chemistry of water seeping from mine-rock piles., in: *Proceedings of the
545 Third International Conference on the Abatement of Acidic Drainage,*
546 *Pittsburgh, Pennsylvania, USA.*

- 547 Morin, K.A., Hutt, N., 1997. Environmental geochemistry of minesite
548 drainage: practical theory and case studies. MDAG Pub.
- 549 Morin, K.A., Hutt, N., 2000. Discrete-zone mixing of net-acid-neutralizing
550 and net-acid-generating rock: Avoiding the argument over appropriate
551 ratios.
- 552 Nichol, C., Smith, L., Beckie, R., 2005. Field-scale experiments of unsatu-
553 rated flow and solute transport in a heterogeneous porous medium. *Water*
554 *Resources Research* 41, W05018. doi:10.1029/2004WR003035.
- 555 Nicholson, R., Gillham, R.W., Reardon, E.J., 1990. Pyrite oxidation in
556 carbonate-buffered solution: 2. Rate control by oxide coatings. *Geochim-*
557 *ica et Cosmochimica Acta* 54, 395–402. doi:10.1016/0016-7037(90)90328-I.
- 558 Nordstrom, D.K., 2011. Hydrogeochemical processes governing the origin,
559 transport and fate of major and trace elements from mine wastes and
560 mineralized rock to surface waters. *Applied Geochemistry* 26, 1777–1791.
561 doi:10.1016/j.apgeochem.2011.06.002.
- 562 Palmer, C.D., Cherry, J.A., 1984. Geochemical evolution of groundwa-
563 ter in sequences of sedimentary rocks. *Journal of Hydrology* 75, 27–65.
564 doi:10.1016/0022-1694(84)90045-3.
- 565 Parbhakar-Fox, A., Lottermoser, B.G., 2015. A critical review of acid rock
566 drainage prediction methods and practices. *Minerals Engineering* 82, 107–
567 124. doi:10.1016/j.mineng.2015.03.015.
- 568 Park, J.Y., Levenspiel, O., 1975. The crackling core model for the re-

569 action of solid particles. *Chemical Engineering Science* 30, 1207–1214.
570 doi:10.1016/0009-2509(75)85041-X.

571 Pedretti, D., Lassin, A., Beckie, R.D., 2015. Analysis of the
572 potential impact of capillarity on long-term geochemical processes
573 in sulphidic waste-rock dumps. *Applied Geochemistry* 62, 75–83.
574 doi:10.1016/j.apgeochem.2015.03.017.

575 Peterson, H.E., 2014. Unsaturated hydrology, evaporation, and geochem-
576 istry of neutral and acid rock drainage in highly heterogeneous mine waste
577 rock at the Antamina Mine, Peru .

578 Price, W., 2009. Prediction manual for drainage chemistry from sulphidic
579 geologic materials.

580 Rahman, M.A., Jose, S.C., Nowak, W., Cirpka, O.A., 2005. Ex-
581 periments on vertical transverse mixing in a large-scale heteroge-
582 neous model aquifer. *Journal of Contaminant Hydrology* 80, 130–148.
583 doi:10.1016/j.jconhyd.2005.06.010.

584 Remy, N., Boucher, A., Wu, J., 2009. *Applied Geostatistics with SGeMS.*
585 *A User’s Guide.* New york cambridge university press. ed.

586 Simmons, C.S., Ginn, T.R., Wood, B.D., 1995. Stochastic-Convective Trans-
587 port with Nonlinear Reaction: Mathematical Framework. *Water Re-*
588 *sources Research* 31, 2675–2688. doi:10.1029/95WR02178.

589 Smith, J., Beckie, R., 2003. Hydrologic and geochemical transport processes
590 in mine waste rock, in: Jambor, J., Blowes, D., Ritchie, A. (Eds.), *Envi-*

591 ronmental aspects of mine wastes. Mineralogical Association of Canada,
592 Ottawa. Short course series, pp. 51–72.

593 Soares, A., 1998. Sequential Indicator Simulation with Correc-
594 tion for Local Probabilities. *Mathematical Geology* 30, 761–765.
595 doi:10.1023/A:1022451504120.

596 Sobek, A.A., Schuller, W.A., Freeman, J.R., Agency, E.P., 1978. Field and
597 laboratory methods applicable to overburdens and minesoils.

598 Strömberg, B., Banwart, S., 1994. Kinetic modelling of geochemical pro-
599 cesses at the Aitik mining waste rock site in northern Sweden. *Applied*
600 *Geochemistry* 9, 583–595. doi:10.1016/0883-2927(94)90020-5.

601 Tartakovsky, D.M., Winter, C.L., 2008. Uncertain future of hydrogeology.
602 *ASCE J. 394 Hydrologic Engrg.* 13, 37–39.

603 Thiele, M., Batycky, R., Blunt, M., Orr, F., 1996. Simulating Flow in Het-
604 erogeneous Systems Using Streamtubes and Streamlines. *SPE Reservoir*
605 *Engineering* 11, 5–12. doi:10.2118/27834-PA.

606 Yabusaki, S.B., Steefel, C.I., Wood, B.D., 1998. Multidimensional,
607 multicomponent, subsurface reactive transport in nonuniform velocity
608 fields: code verification using an advective reactive streamtube approach.
609 *Journal of Contaminant Hydrology* 30, 299–331. doi:10.1016/S0169-
610 7722(97)00050-8.